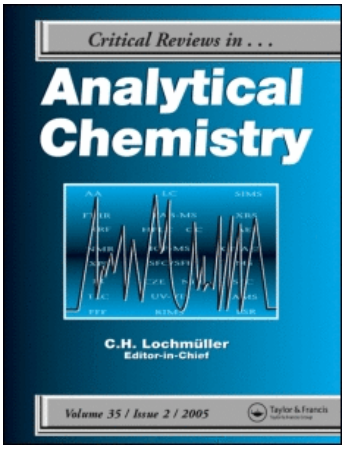

Critical Reviews in Analytical Chemistry
Publication details, including instructions for authors and subscription information:
http://www.informaworld.com/smpp/title~content=t713400837

Making Reference Samples Redundant

Mikael Kubista; Jan Nygren; Abdalla Elbergali; Robert Sjöback

Online publication date: 03 June 2010

To cite this Article Kubista, Mikael , Nygren, Jan , Elbergali, Abdalla and Sjöback, Robert(1999) 'Making Reference Samples Redundant', Critical Reviews in Analytical Chemistry, 29: 1, 1 — 28
To link to this Article: DOI: 10.1080/10408349891199275
URL: http://dx.doi.org/10.1080/10408349891199275

Critical Reviews in Analytical Chemistry, 29(1):1–28 (1999)

Making Reference Samples Redundant

Mikael Kubista, Jan Nygren, Abdalla Elbergali, and Robert Sjöback

Department of Biochemistry and Biophysics, Chalmers University of Technology, SE-413 90 Gothenburg, Sweden

ABSTRACT: Chemometric methods to analyze spectroscopic data without using reference spectra are discussed. The data are first decomposed into principal components, and the number of contributing species is determined by statistical tests. The principal components are then rotated to produce spectroscopic responses and concentration profiles of the chemical species present. Samples that vary in a physical property like pH, total concentration, temperature, or ionic strength, are analyzed by regular 1-dimensional spectroscopy assuming that the components are in chemical equilibrium. Samples containing noninteracting compounds are analyzed by multidimensional spectroscopy, and the principal components are calculated by Procrustes rotation. Several applications of the two approaches on absorption and fluorescence data are presented.

KEY WORDS: chemometrics, spectroscopy, fluorescence, UV-VIS, procrustes rotation, physical constraints, equilibrium.

I. INTRODUCTION

The prime goal when analyzing test samples is to determine the number of components they contain, identify the components, and optionally to determine their concentrations. This usually requires that the components be separated, which is a tedious process that may not always be feasible. By spectroscopy, components in a test sample may be identified by comparing the measured spectrum with those of standards. If standards are not available, the common belief has been that the components' spectral responses cannot be separated, which precludes their identification. However, as discussed here, modern multivariate approaches, in combination with rational experimental design, open some powerful means to characterize test samples with minimum assumptions. These methods are today commonly known as chemometrics — a word coined in 1971 by the Swedish chemist Svante Wold — which refers to the applications of mathematical and statistical methods to solve chemical problems. A large number of chemometric methods is available today. In this review we focus on the methods developed in our group that do not require reference spectra.

The first serious attempt to analyze spectroscopic data using multivariate methods was made in 1971 by Lawton and Sylvestre.[1] They showed that it was not possible to obtain an unambiguous result when analyzing sets of regular 1-dimensional spectra, and provided a self-modeling curve resolution (SMCR) method to estimate a solution range for the components' spectral responses and concentrations assuming nonnegative responses. Their approach was later generalized to more components.[2] However, experi-

mental data contain noise that may cause some data points to be negative, and stringent application of the non-negative criterion may disqualify the correct solution.

In 1990, our group found a way to remove the solution ambiguity. By a strategic experimental design that generated multidimensional data suitable for analysis by Procrustes rotation, we showed it was possible to determine components' spectral responses and their relative concentrations in a series of test samples without making assumptions about spectral shapes and without using references.[3,4] This approach has been shown to be mathematically equivalent to the generalized rank annihilation method by Sanches and Kowalski[5] that was originally developed to compare test data with those of a standard set. The Procrustes rotation method has later been used to characterize pairs of samples by two-dimensional spectroscopy,[6,7] and it can also characterize a single sample by a 3-dimensional measurement. As a complement to the Procrustes rotation method, the physical constraint approach was developed to determine spectral responses and relative concentrations of components that are in chemical equilibrium. The analysis is applicable to regular 1-dimensional spectra and it is particularly useful to study equilibria where some of the components cannot be obtained in pure form. It was initially applied to two-component equilibria,[8] but is readily applicable also on multicomponent systems.[9] Particularly interesting are approaches based on temperature variations, which can be applied on individual test samples.[10] In this review, we describe both the Procrustes rotation and the physical constraint approaches and demonstrate their applicability by several examples.

II. DETERMINING THE NUMBER OF COMPONENTS IN THE SAMPLES

The first problem encountered when analyzing test samples spectroscopically is to determine the number of components that they contain. Only those components that contribute to the recorded spectra can be distinguished. If two species, A and B, interact to form a complex AB, the number of components is three: A, B, and AB. If both A and B contribute to the recorded spectra and their spectral responses change upon complex formation so that the spectrum of AB is different from the sum of the A and B spectra, all three species can be distinguished. But if only A or only B contributes to the spectra, or the spectrum of AB is the sum of the A and B spectra, only two of the components are independent. The relative concentrations of the components must also differ among the samples. For example, two protolytic species are readily distinguished in a pH titration, while their contributions can not be separated in samples that have the same pH. The number of components that can be distinguished is the same as the number of independent spectra that accounts for all systematic variations in the experimental data, and can be determined by a procedure known as principal component analysis, PCA.[11]

III. PRINCIPAL COMPONENT ANALYSIS

In PCA the recorded spectra are arranged as rows in an $(n \times m)$ data matrix, **A**, where n is the number of recorded spectra and m is the number of data points collected per spectrum. Matrix **A** is then decomposed into an orthonormal basis set (Figure 1):

$$\mathbf{A} = \mathbf{T}_{n\times q}\mathbf{P}'_{q\times m} = \sum_{i=1}^{q} \mathbf{t}_i\mathbf{p}'_i \qquad \text{where } q = \min(n, m) \tag{1}$$

$\mathbf{T}_{n\times q}$ is an $n \times q$ matrix whose columns, $\mathbf{t}_i$, are referred to as target vectors. The nor-

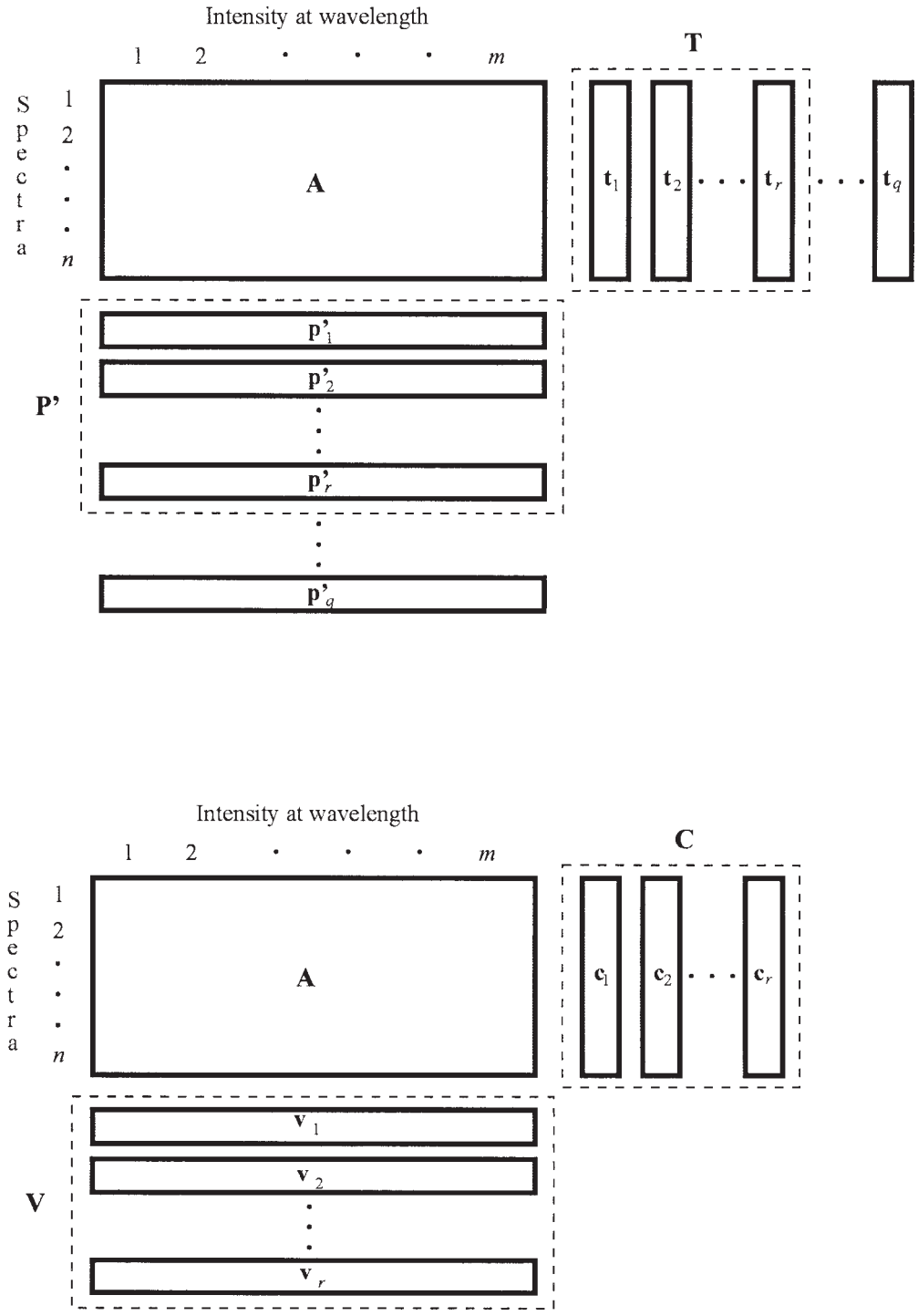

FIGURE 1. *Top:* Principal component decomposition of data matrix **A** into a product of a target (**T**) and a projection (**P**) matrix. *Bottom:* Relation between the data matrix **A** and the concentration (**C**) and spectral response (**V**) matrices.

malized target vectors are the eigenvectors of matrix $\mathbf{AA}'$, which is the $n \times n$ square covariance matrix obtained by post-multiplying **A** by its transpose. Their lengths are the eigenvalues of $\mathbf{AA}'$. The target vectors are orthogonal

$$\mathbf{t}_i\mathbf{t}'_j = \sum_{k=1}^{n} t_{ki}t_{kj} = 0 \quad (i \neq j) \tag{2}$$

$\mathbf{P}'$ is an $(q \times m)$ matrix whose rows, $\mathbf{P}'_i$, are referred to as projection vectors. The projection vectors are eigenvectors to matrix $\mathbf{A}'\mathbf{A}$ and they are orthonormal:

$$\begin{aligned} \mathbf{p}_i\mathbf{p}'_j &= \sum_{k=1}^{m} (p')_{ik}(p')_{jk} = 0 \quad (i \neq j) \\ \mathbf{p}_i\mathbf{p}'_i &= \sum_{k=1}^{m} (p')_{ik}(p')_{ik} = 1 \end{aligned} \tag{3}$$

The target and the projection vectors are called the principal components (PCs) of matrix **A**.

A. The r Most Significant PCs Account for the Spectral Features

Figure 2 shows a set of absorption spectra of fluorescein at different pH in the interval 2.0 to 9.5. The spectra are decomposed into principal components and the four most significant are shown in Figure 3. The projection vectors have distinct spectral features and the target vectors vary systematically with pH, suggesting that they reflect features of the sample components. The relevance of the PCs can be tested by reproducing the spectra:

$$\tilde{\mathbf{A}}_l = \sum_{i=1}^{i} \mathbf{t}_i\mathbf{p}'_i \tag{4}$$

where $\tilde{\mathbf{A}}_i$ is the data matrix reconstructed from the l most significant PCs. Figure 4 shows the reconstructed spectra from 1 to 4 of the most significant PCs and compares them with the measured spectra. When three or less PCs are used the residuals are substantial and clearly non-random, while with four PCs the difference between the reproduced and measured spectra is negligible. This tells us that four fluorescein species contribute to the measured spectra. These

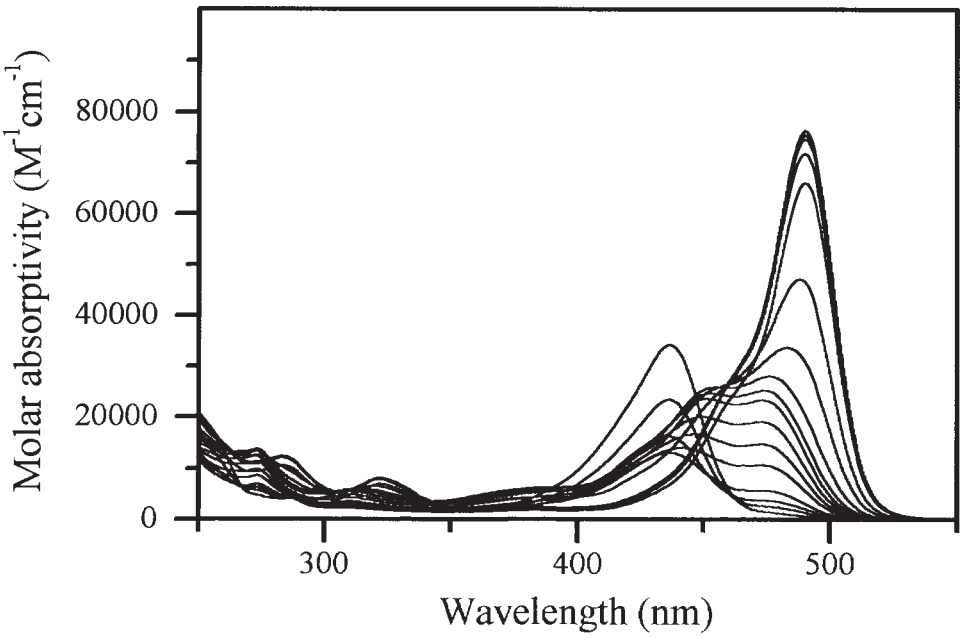

FIGURE 2. Absorption spectra of fluorescein recorded in the pH interval 2.0 to 9.5. The intensity at 490 nm increases with increasing pH.

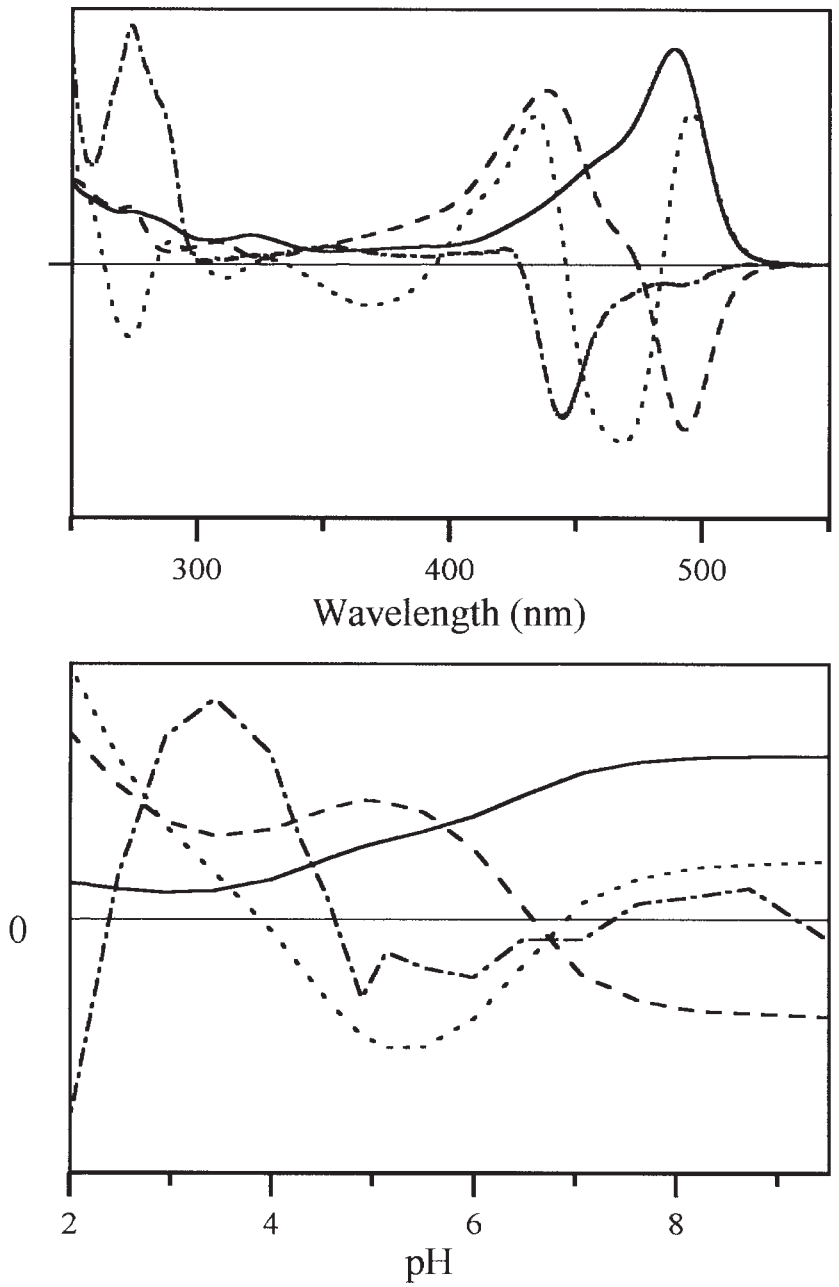

FIGURE 3. The four most significant principal components. Projection vectors are shown in the top panel and target vectors in the bottom panel. The principal components are shown normalized for clarity.

have been shown to be the cation, neutral species, anion and dianion.[6]

The number of significant components that contribute to the spectra can also be determined by statistical means. Elbergali et al. compared a number of statistical tests and found the factor indicator function (IND) to perform best for spectroscopic data.[12]

$$\mathrm{IND}(l) = \frac{\sqrt{\left[\dfrac{\sum_{j=l+1}^{q} g_j}{n(q-l)}\right]}}{(q-l)^2} \tag{5}$$

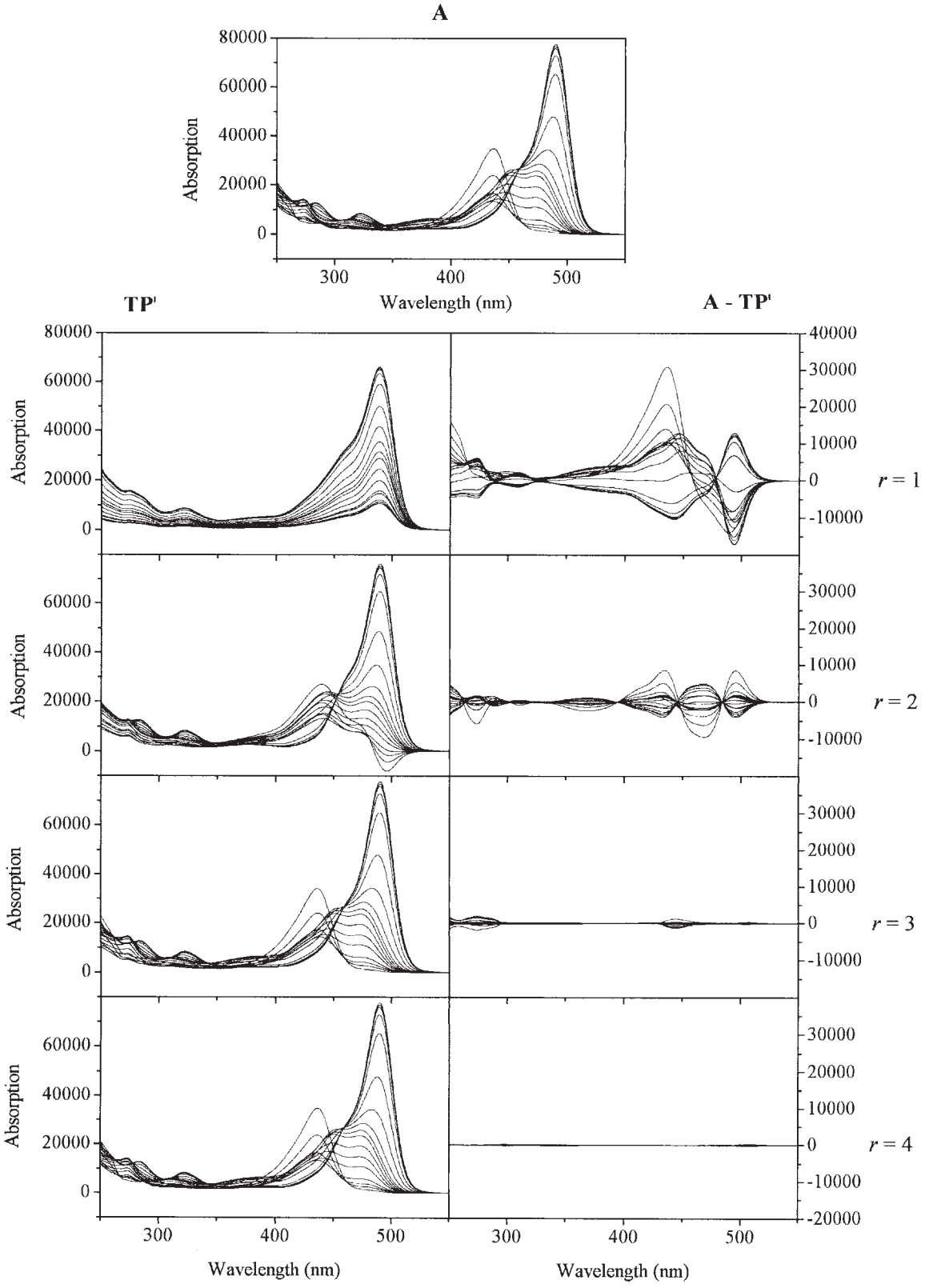

FIGURE 4. *Top:* Experimental spectra. *Bottom:* Reproduced spectra and the residual between the experimental and reproduced spectra when using (top to bottom) 1 to 4 principal components.

where g_j are the eigenvalues defined as

$$g_j = \sum_{i=1}^{q} t_{ij}^2 \quad (j = 1,2,\ldots,r,\ldots,q) \quad (6)$$

and q is the least of n and m. IND(l) decreases steeply with increasing l as long as significant PCs are included and when these are exhausted IND(l) levels off. This point, at which $r = l$, is most readily recognized from the second or third derivative of the indicator function, which have extreme points. The minimum of the third derivative at $l = 4$ in Figure 5 shows that four compo-

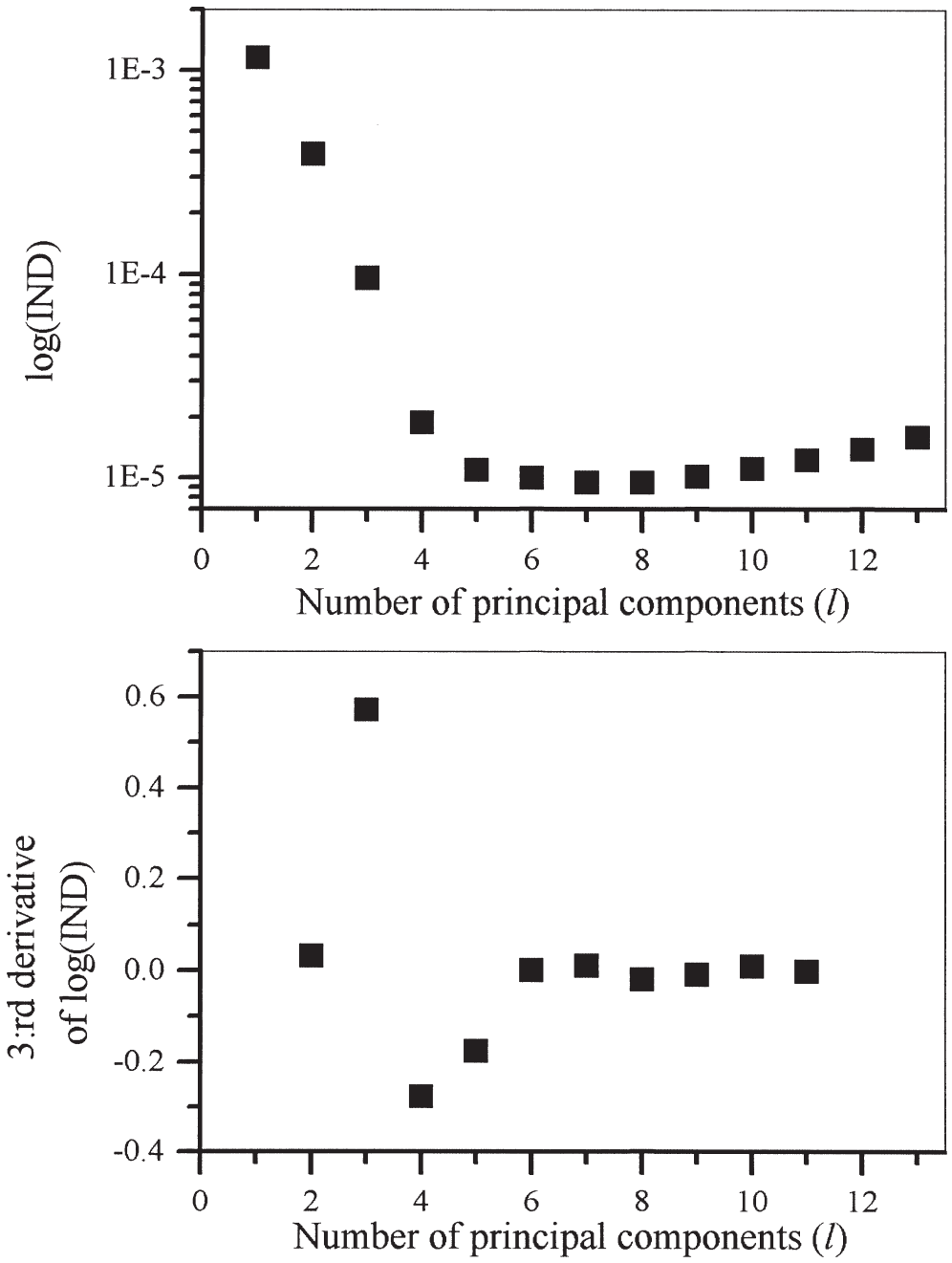

FIGURE 5. *Top:* Logarithm of the indicator as a function of the number of PCs used in data reconstruction. *Bottom:* Third derivative of the indicator function.

nents contribute to the spectra in the previous example.

The noise in the reproduced spectra is considerably lower than in the experimental ones. The reason is that the insignificant PCs that contain most of the noise have been left out in the reproduction. To decompose a data set into principal components and then reproduce the data from the most significant PCs is in fact one of the most efficient ways to reduce experimental noise. In general:

$$\mathbf{A} = \mathbf{E} + \mathbf{T}_{n\times r}\mathbf{P}'_{r\times m} \approx \sum_{i=1}^{r} \mathbf{t}_i\mathbf{p}'_i = \tilde{\mathbf{A}} \quad (7)$$

where $\mathbf{T}_{n\times r}$ is an $(n \times r)$ matrix having the r most significant target vectors as columns and $\mathbf{P}'_{r\times m}$ is an $(r \times m)$ matrix having the r most significant projection vectors as rows, r is the number of distinguishable components that contribute to the spectra and **E** is the error matrix containing the noise that is left out of the reproduction. In the following we shall drop the subscripts on **T** and **P′** and assume that they refer to submatrices containing the r most significant PCs.

B. NIPALS Decomposition

Calculating the eigenvalues of the **AA′** and **A′A** matrices to determine the PCs is rather time consuming for the large data sets usually encountered in spectroscopy. The PCs may instead be calculated iteratively using the Nonlinear Iterative Partial Least Squares (NIPALS) algorithm.[13] By NIPALS, the PCs are extracted pair-wise in the order of decreasing significance, and the calculation can be terminated after any number of iterations. Because the number of components (r) in general is much smaller than the number of samples (n), NIPALS may save considerable execution time. NIPALS can also readily be combined with the statistical tests. After each iteration, yielding a new pair of PCs, the indicator and its derivative are evaluated. When an extreme point in the derivative is encountered $l = r$ and the iteration is terminated.[12]

C. Relation between the Principal Components and the Specific Responses of the Sample Components

The principal components are abstract factors that cannot directly be correlated to physical properties of the sample components. For spectra recorded on a series of samples, such as those in Figure 2, the target vectors are related to the components' concentrations and the projection vectors to the components' spectral responses. Assuming linear response, the recorded spectra are related to the components' concentrations as

$$\mathbf{a}_i(\lambda) = \sum_{j=1}^{r} \mathbf{c}_{ij}\mathbf{v}_j(\lambda) + \mathbf{e}_i(\lambda) \quad (i = 1, n) \quad (8)$$

where c_{ij} is the concentration of component j in sample i, $\mathbf{v}_j(\lambda)$ is the normalized response of component j and $\mathbf{e}_i(\lambda)$ is the experimental error. λ indicates that the spectra are recorded as a function of wavelength. In matrix notation (Figure 1):

$$\mathbf{A} = \mathbf{CV} + \mathbf{E}_\mathbf{A} \approx \mathbf{CV} = \sum_{j=1}^{r} \mathbf{c}_j\mathbf{v}_j \quad (9)$$

where **C** is an $(n \times r)$ matrix containing the components' concentrations as columns and **V** is an $(r \times m)$ matrix containing the components' spectra as rows. Comparing Eqs. 7 and 9:

$$\mathbf{A} \approx \mathbf{CV} \approx \mathbf{TP}' \quad (10)$$

C is in general not equal to **T** and **V** is not equal to **P′**. The matrices are related through a rotation, which can be realized by inserting

an arbitrary square ($r \times r$) rotation matrix $\tilde{\mathbf{R}}$ times its inverse:

$$\mathbf{CV} \approx \mathbf{TP}' = \mathbf{T}\left(\tilde{\mathbf{R}}^{-1}\tilde{\mathbf{R}}\right)\mathbf{P}' = \left(\mathbf{T}\tilde{\mathbf{R}}^{-1}\right)\left(\tilde{\mathbf{R}}\mathbf{P}'\right) \quad (11)$$

where the tilde indicates a nonconstrained matrix. The product of the target and projection matrices is not a unique solution to Eq. (10), but any linear combination of the target vectors multiplied with a reciprocal linear combination of the projection vectors is a mathematically equally acceptable solution. To determine which of these degenerate solutions is correct one must invoke constraints. The problem can then be defined as finding the rotation matrix **R** that under a particular set of constraints best satisfies:

$$\mathbf{C} \approx \mathbf{TR}^{-1} \quad (12)$$

$$\mathbf{V} \approx \mathbf{RP}' \quad (13)$$

IV. PHYSICAL CONSTRAINTS

The physical constraint approach is applicable to samples that contain components that are in chemical equilibrium. The samples must differ in a physical property, such as pH, volume, temperature, pressure, ionic strength, etc., that in a predictable way affects the concentrations of the components. A single 1-dimensional spectrum recorded on each sample is sufficient for analysis. The components' spectral responses do not need to be known in advance, but if some are the information can be used as additional constraint. The thermodynamic expression that describes the components' concentrations is the main constraint used to determine **R**, from which thermodynamic parameters and components' spectral responses and concentrations are calculated.

The strategy is as follows. The components' concentrations are expressed as functions of the thermodynamic parameters (**K**) and the physical property (Π) that differentiates the samples:

$$c_{ij}\left(\Pi_i\right) = f\left(\Pi_i, \mathbf{K}\right) \quad \left(i = 1,n;\ j = l,r\right) \quad (14)$$

where Π_i is the value of the physical parameter in sample i and **K** is a vector containing the thermodynamic parameters that describe the system. The Π_i:s are known, while the **K**:s are not. A set of trial component concentrations is first calculated for a set of trial values of the thermodynamic parameters,

$$\tilde{c}_{ij}\left(\Pi_i\right) = f\left(\Pi_i, \tilde{\mathbf{K}}\right) \quad \left(i = 1,n;\ j = l,r\right) \quad (15)$$

the trial concentrations are fitted to the target vectors:

$$\mathbf{t}_k = \sum_{j=1}^{r} \tilde{\mathbf{c}}_j \tilde{\mathbf{r}}_{jk} \quad (16)$$

and the goodness of the fit is evaluated by calculating the sum of square residuals:

$$\chi^2 = \sum_{i=1}^{n} \sum_{k=1}^{r} \left(t_{ik} - \sum_{j=1}^{r} \tilde{c}_{ij} \tilde{r}_{jk} \right)^2 \quad (17)$$

The set of trial values of the thermodynamic parameters that produces the least χ^2 is considered correct. A number of examples follows.

A. pH Titrations

Principal component analysis of the fluorescein absorption spectra in Figure 2 revealed the presence of four species, which are the cation, neutral species, anion, and dianion.[6] They are involved in the protolytic equilibria:

$$\mathrm{HFl^-} \xleftrightarrow{K_3} \mathrm{H^+ + Fl^{2-}}$$

$$\mathrm{H_2Fl^-} \xleftrightarrow{K_2} \mathrm{H^+ + HFl^-}$$

$$\mathrm{H_3Fl^+} \xleftrightarrow{K_1} \mathrm{H^+ + H_2Fl}$$

and their concentrations are related as:

$$\frac{[H_2Fl]\{H^+\}}{[H_3Fl^+]} = K_1 \quad (18)$$

$$\frac{[HFl^-]\{H^+\}}{[H_2Fl]} = K_2 \quad (19)$$

$$\frac{[Fl^{2-}]\{H^+\}}{[HFl^-]} = K_3 \quad (20)$$

This can be rearranged to:

$$\mathbf{c}_{H_3Fl^+} = \frac{\mathbf{c}^3_{H^+}}{\mathbf{c}^3_H + K_1\mathbf{c}^2_{H^+} + K_1K_2\mathbf{c}_{H^+} + K_1K_2K_3} c_{tot} \quad (21)$$

$$\mathbf{c}_{H_3Fl} = \frac{K_1\mathbf{c}^2_{H^+}}{\mathbf{c}^3_H + K_1\mathbf{c}^2_{H^+} + K_1K_2\mathbf{c}_{H^+} + K_1K_2K_3} c_{tot} \quad (22)$$

$$\mathbf{c}_{HFl^-} = \frac{K_1K_2\mathbf{c}_{H^+}}{\mathbf{c}^3_H + K_1\mathbf{c}^2_{H^+} + K_1K_2\mathbf{c}_{H^+} + K_1K_2K_3} c_{tot} \quad (23)$$

$$\mathbf{c}_{Fl^{2-}} = \frac{K_1K_2K_3}{\mathbf{c}^3_H + K_1\mathbf{c}^2_{H^+} + K_1K_2\mathbf{c}_{H^+} + K_1K_2K_3} c_{tot} \quad (24)$$

where K_1, K_2, and K_3 are the three protolytic constants, and $\mathbf{c}_{H_3Fl^+}$, $\mathbf{c}_{H_2Fl^-}$, $\mathbf{c}_{HFl^-}$, $\mathbf{c}_{Fl^{2-}}$, and $\mathbf{c}_{tot}$ are vectors containing the concentrations of the fluorescein species. If the total fluorescein concentration, c_{tot}, is unknown, it is arbitrarily set to 1 and relative concentrations of the fluorescein species are calculated. The vectors $\mathbf{c}_{H^+}$, $\mathbf{c}^2_{H^+}$, and $\mathbf{c}^3_{H^+}$ contain the proton activities and the square and cube of the proton activities. These are measured through pH. The protolytic constants are determined by a grid search. For various trial values of the protolytic constants, sets of trial concentration vectors are calculated and fitted to the target vectors:

$$\mathbf{t}_1 = \tilde{r}_{11}\tilde{c}_{H_3Fl^+} + \tilde{r}_{21}\tilde{\mathbf{c}}_{H_2Fl} + \tilde{r}_{31}\tilde{\mathbf{c}}_{HFl^-} + \tilde{r}_{41}\tilde{\mathbf{c}}_{F^{2-}} \quad (25)$$

$$\mathbf{t}_2 = \tilde{r}_{12}\tilde{c}_{H_3Fl^+} + \tilde{r}_{22}\tilde{\mathbf{c}}_{H_3Fl} + \tilde{r}_{32}\tilde{\mathbf{c}}_{HFl^-} + \tilde{r}_{42}\tilde{\mathbf{c}}_{F^{2-}} \quad (26)$$

$$\mathbf{t}_3 = \tilde{r}_{13}\tilde{c}_{H_2Fl^+} + \tilde{r}_{23}\tilde{\mathbf{c}}_{H_2Fl} + \tilde{r}_{33}\tilde{\mathbf{c}}_{HFl^-} + \tilde{r}_{43}\tilde{\mathbf{c}}_{F^{2-}} \quad (27)$$

$$\mathbf{t}_4 = \tilde{r}_{14}\tilde{c}_{H_3Fl^+} + \tilde{r}_{24}\tilde{\mathbf{c}}_{H_2Fl} + \tilde{r}_{34}\tilde{\mathbf{c}}_{HFl^-} + \tilde{r}_{44}\tilde{\mathbf{c}}_{F^{2-}} \quad (28)$$

For each fit χ^2 is calculated and the set of protolytic constants that produces the best fit is considered correct. Figure 6 shows subsections of the χ^2 surface, which has a global minimum at $pK_1 = 2.1$, $pK_2 = 4.3$, and $pK_3 = 6.41$. From the surface, one can conclude that pK_2 and pK_3 are determined with considerably higher accuracy than pK_1.[9] The **R** matrix that produces the best fit is used to calculate the components' spectral responses and concentrations (Figure 7).

B. Concentration Titrations

Interaction between species can be studied by varying their relative concentrations. The simplest system is the dimerization equilibrium:

$$2\mathbf{A} \xleftrightarrow{K_D} \mathbf{A}_2$$

which can be characterized by varying the total concentration of the species of interest. This is illustrated in Figure 8 for benzoic acid characterized by absorption spectroscopy. With increasing concentration of benzoic acid, the spectrum shifts to lower wavelength owing to dimer formation. The concentrations of the benzoic acid monomer and dimer are related:

$$K_D = \frac{c_{A_2}}{c^2_A} \quad (29)$$

$$c_A + 2c_{A_2} = c_{tot} \quad (30)$$

and can be expressed as a function the total benzoic acid concentration and the dimerization constant:

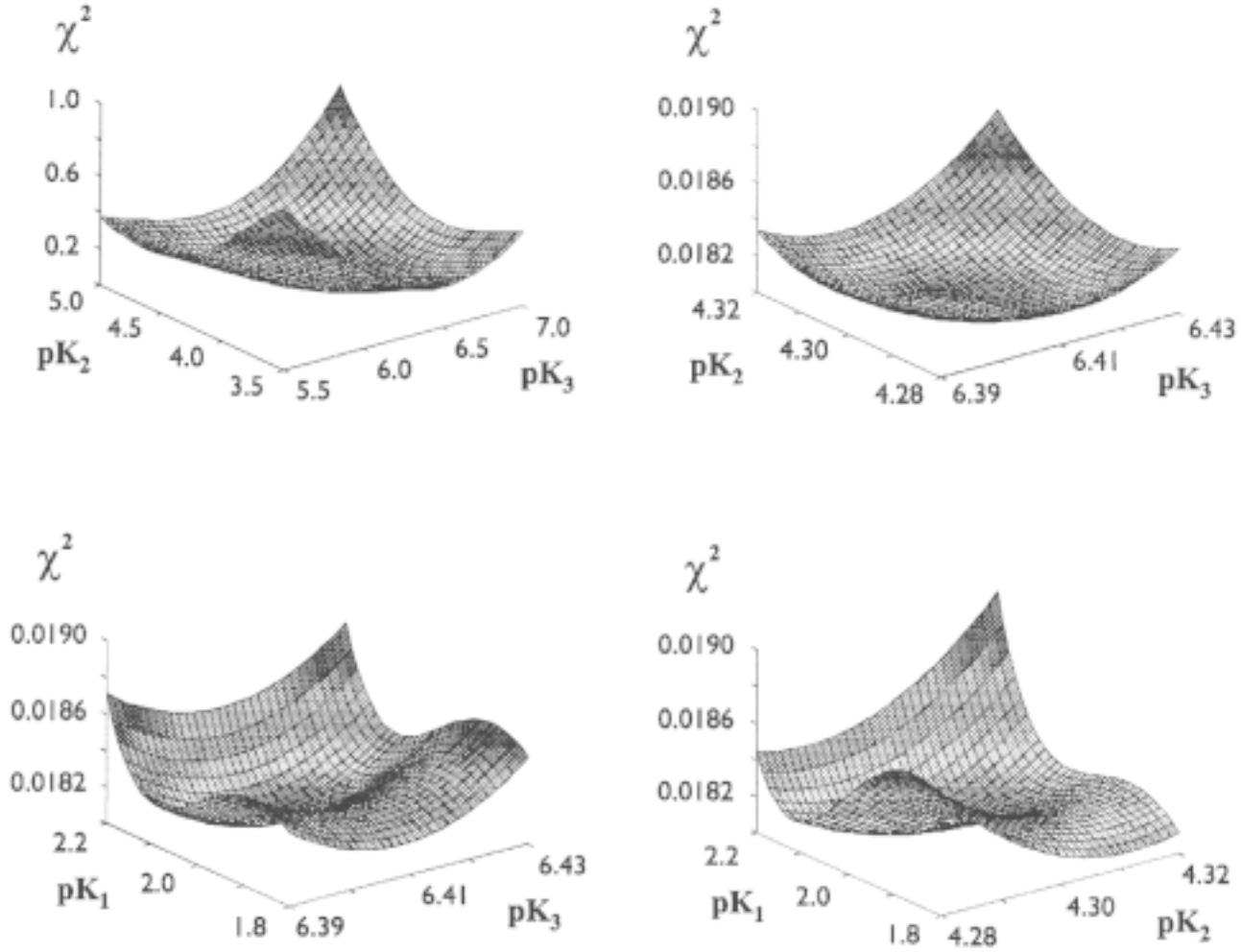

FIGURE 6. Subsections of the χ^2 surface. *Top left:* dependence on pK_2 and pK_3 for $pK_1 = 2.1$. *Top right:* Enlargement of the subsurface showing the dependence on pK_2 and pK_3 for $pK_1 = 2.1$. *Bottom left:* dependence on pK_1 and pK_3 for $pK_2 = 4.3$. *Bottom right:* dependence on pK_1 and pK_2 for $pK_3 = 6.41$.

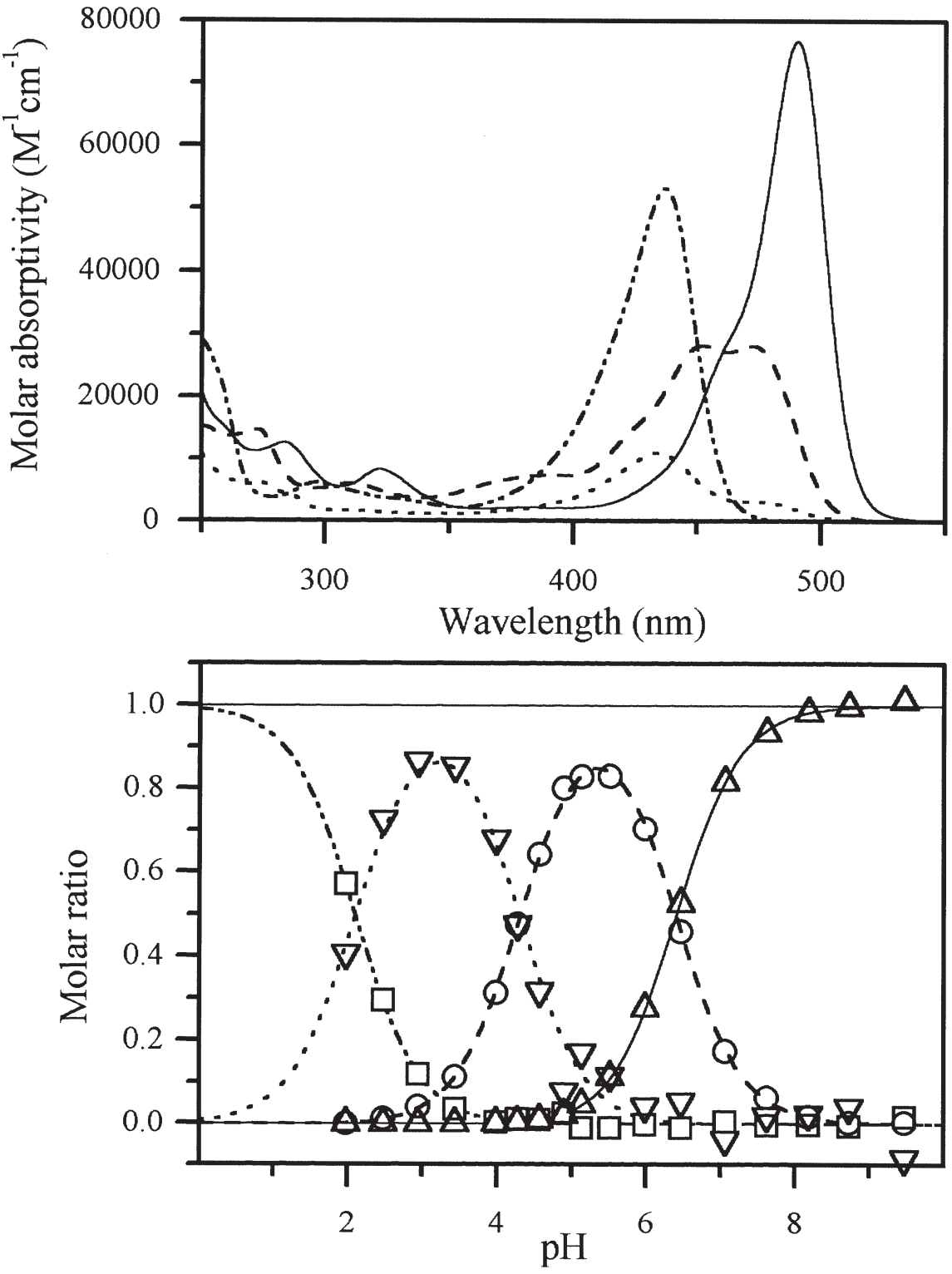

FIGURE 7. Calculated spectra (*top*) and concentrations (*bottom*) of the fluorescein protolytic species.

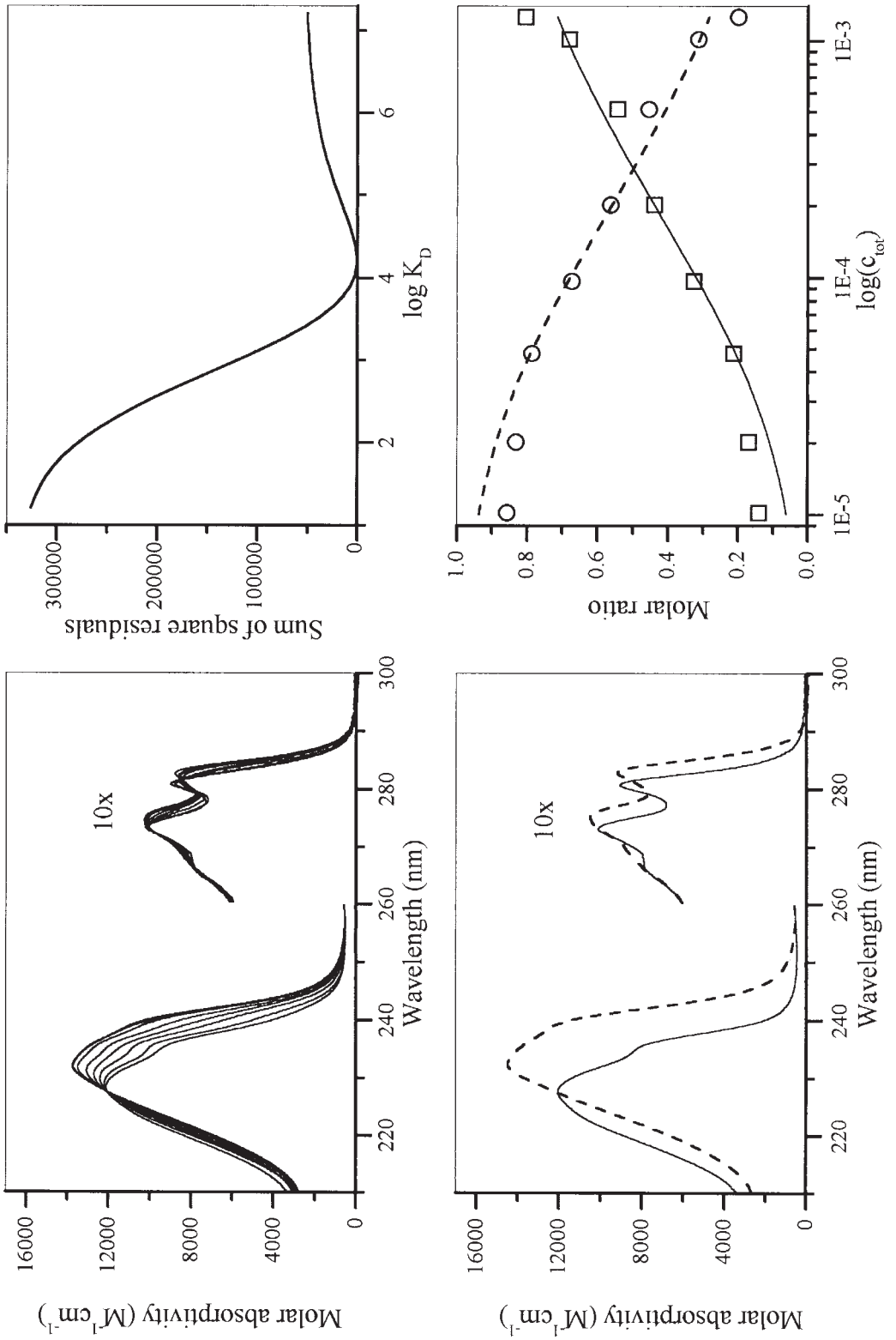

FIGURE 8. *Top left:* Normalized absorption spectra of benzoic acid recorded at different total concentration. *Top right:* χ^2 dependence on log K_D. Calculated absorption spectra (*bottom left*) and concentrations (*bottom right*) of the benzoic acid monomer and dimer.

$$c_A = -\left(4K_D\right)^{-1} \underset{(-)}{+} \sqrt{\left(4K_D\right)^{-2} + \frac{c_{tot}}{2K_D}} \qquad (31)$$

$$c_{A_2} = \frac{c_{tot} + \left(4K_D\right)^{-1}}{2} \underset{-}{(+)} \sqrt{\left(\frac{c_{tot}\left(4K_D\right)^{-1}}{2}\right)^2 - \frac{c_{tot}^2}{4}} \qquad (32)$$

Trial concentrations vectors, $\tilde{\mathbf{c}}_A$ and $\tilde{\mathbf{c}}_{A_2}$, are calculated for different trial values of K_D and fitted to the two most significant target vectors determined by PCA:

$$\mathbf{t}_1 = \tilde{r}_{11}\tilde{\mathbf{c}}_A + \tilde{r}_{21}\tilde{\mathbf{c}}_{A_2} \qquad (33)$$

$$\mathbf{t}_2 = \tilde{r}_{12}\tilde{\mathbf{c}}_A + \tilde{r}_{22}\tilde{\mathbf{c}}_{A_2} \qquad (34)$$

Figure 8 shows the χ^2 dependence on K_D (top right). The minimum at $K_D = 15.9 \times 10^3$ M^{-1} defines an **R** matrix from which the spectral responses (bottom left) and concentrations (bottom right) of the benzoic acid species can be calculated.

C. Temperature Titrations

Thermodynamic equilibrium constants depend on temperature as predicted by the van't Hoff's equation:

$$\ln K(T) = \frac{1}{R}\left(\Delta S^{\varnothing} - \frac{\Delta H^{\varnothing}}{T}\right) \qquad (35)$$

where $\Delta H^{\varnothing}$ is the molar enthalpy change, $R = 8.31$ $Jmol^{-1}K^{-1}$ is the universal gas constant, and T is the Kelvin temperature. This can be used as a constraint to characterize chemical equilibria by studying the spectral changes induced by temperature. Again with benzoic acid as example:

$$K_D(T) = \frac{c_{A_2}(T)}{\left(c_{A_2}(T)\right)^2} \qquad (36)$$

$$c_A(T) + 2c_{A_2}(T) = c_{tot} \qquad (37)$$

where both K_D and concentrations now depend on temperature. Matrix **R**, which relates the concentrations to the target vectors, has the elements:

$$\mathbf{R} = \begin{bmatrix} r_{11} & r_{12} \\ r_{21} & r_{22} \end{bmatrix} \qquad (38)$$

Its inverse is:

$$\mathbf{R}^{-1} = \frac{1}{r_{11}r_{22} - r_{21}r_{12}} \begin{bmatrix} r_{22} & -r_{12} \\ -r_{21} & r_{11} \end{bmatrix} \qquad (39)$$

Combining Eqs. 12, 37, and 39

$$\frac{1}{r_{11}r_{22} - r_{12}r_{21}}\left(\mathbf{t}_1 r_{22} - \mathbf{t}_2 r_{21} - 2\mathbf{t}_1 r_{12} + 2\mathbf{t}_2 r_{11}\right) = \mathbf{c}_{tot} \qquad (40)$$

which can be written

$$f_{11}\mathbf{t}_1 + f_{12}\mathbf{t}_2 = \mathbf{c}_{tot} \qquad (41)$$

where

$$f_{11} = \left(r_{22} - 2r_{12}\right)\left(r_{11}r_{22} - r_{12}r_{21}\right)^{-1} \qquad (42)$$

and

$$f_{12} = \left(2r_{11} - r_{21}\right)\left(r_{11}r_{22} - r_{12}r_{21}\right)^{-1} \qquad (43)$$

f_{11} and f_{12} are determined by fitting the two target vectors to a vector $\mathbf{c_{tot}}$ with all elements equal to c_{tot}. This gives two relations between the elements of matrix **R**, making two of its elements redundant. In principle,

the two remaining elements of **R** can be determined by finding the combination of $\Delta H^{\varnothing}$ and $\Delta S^{\varnothing}$ trial values that produces the best fit of $\ln K_D(T)$ vs. $1/T$. Such an analysis is, however, quite unstable.[10] Improved stability is achieved if the spectrum of one of the components can be recorded separately and used as additional constraint. For the benzoic acid system, the spectrum of the benzoic acid monomer can be measured in a highly diluted solution. Normalizing the monomer spectrum to the same total concentration as the test sample, it is fitted to the two most significant projection vectors:

$$\mathbf{v}_{\mathbf{monomer}} = r_{11}\mathbf{p}'_1 + r_{12}\mathbf{p}'_2 = f_{21}\mathbf{p}'_1 + f_{22}\mathbf{p}'_2 \quad (44)$$

where $f_{21} = r_{11}$ and $f_{22} = r_{12}$ provide another two relations between the elements of matrix **R**. These are, however, not independent of f_{11} and f_{12}, and the four regression coefficients cannot be combined to solve for all the elements of matrix **R**.[14] However, they can be combined to express **R** in a single element, below arbitrarily chosen to be r_{21}:

$$\mathbf{R} = \begin{bmatrix} f_{21} & f_{22} \\ r_{21} & 2f_{22} + (2f_{21} - r_{21})\dfrac{f_{11}}{f_{12}} \end{bmatrix} \quad (45)$$

Defined this way, matrix **R** produces **C** and **V** matrices that are consistent with the known total concentration of the benzoic acid and the known spectral response of the benzoic acid monomer; the value of r_{21} only affects the dimer spectrum and the monomer concentration profile. For arbitrary values of r_{21}, trial **R** matrices are constructed from which trial concentration profiles are calculated and combined to give trial equilibrium constants. Linear regressions of $\ln K_D(T)$ vs. $1/T$ are then performed and evaluated by calculating χ^2. Best fit determines $\Delta H^{\varnothing}$ and $\Delta S^{\varnothing}$, and from the corresponding **R** matrix components' spectral responses and concentrations are calculated (Figure 9).

D. Ionic Strength Titrations

Equilibria between charged species, such as cationic ligands and nucleic acids, are readily characterized by ionic strength titrations.

$$\mathrm{N} + \mathrm{L_f} \xleftrightarrow{K} \mathrm{NL_b}$$

and

$$K(I) = \frac{[\mathrm{NL_b}]}{[\mathrm{N}][\mathrm{L_f}]} \quad (46)$$

where [N] is the concentration of the nucleic acid expressed in bases or base pairs and $[L_f]$ and $[NL_b]$ are the concentrations of free and bound ligand, respectively. In monovalent salts the logarithm of the equilibrium constant decreases linearly with the logarithm of the ionic strength:[15]

$$\log K(I) = a - b \log I \quad (47)$$

where a is the logarithm of the affinity constant in 1 M salt and b depends on the number of released counterions upon ligand binding. In the analysis a and b are treated as adjustable parameters.[17] The total concentration of ligand

$$c_{\mathrm{f}}(I) + c_{\mathrm{b}}(I) = c_{\mathrm{tot}} \quad (48)$$

and the spectrum of free ligand, $\mathbf{v}_f(\lambda)$, measured separately, are fitted to the two most significant target and projection vectors, respectively, and used as additional constraint to produce the matrix **R**:

$$\mathbf{R} = \begin{bmatrix} f_{21} & f_{22} \\ r_{21} & f_{22} + (f_{21} - r_{21})\dfrac{f_{11}}{f_{12}} \end{bmatrix} \quad (49)$$

Linear regression of $\log(K)$ with respect to $\log(I)$ is performed for various trial values of r_{21} and evaluated by calculating χ^2. The approach is illustrated in Figure 10 by deter-

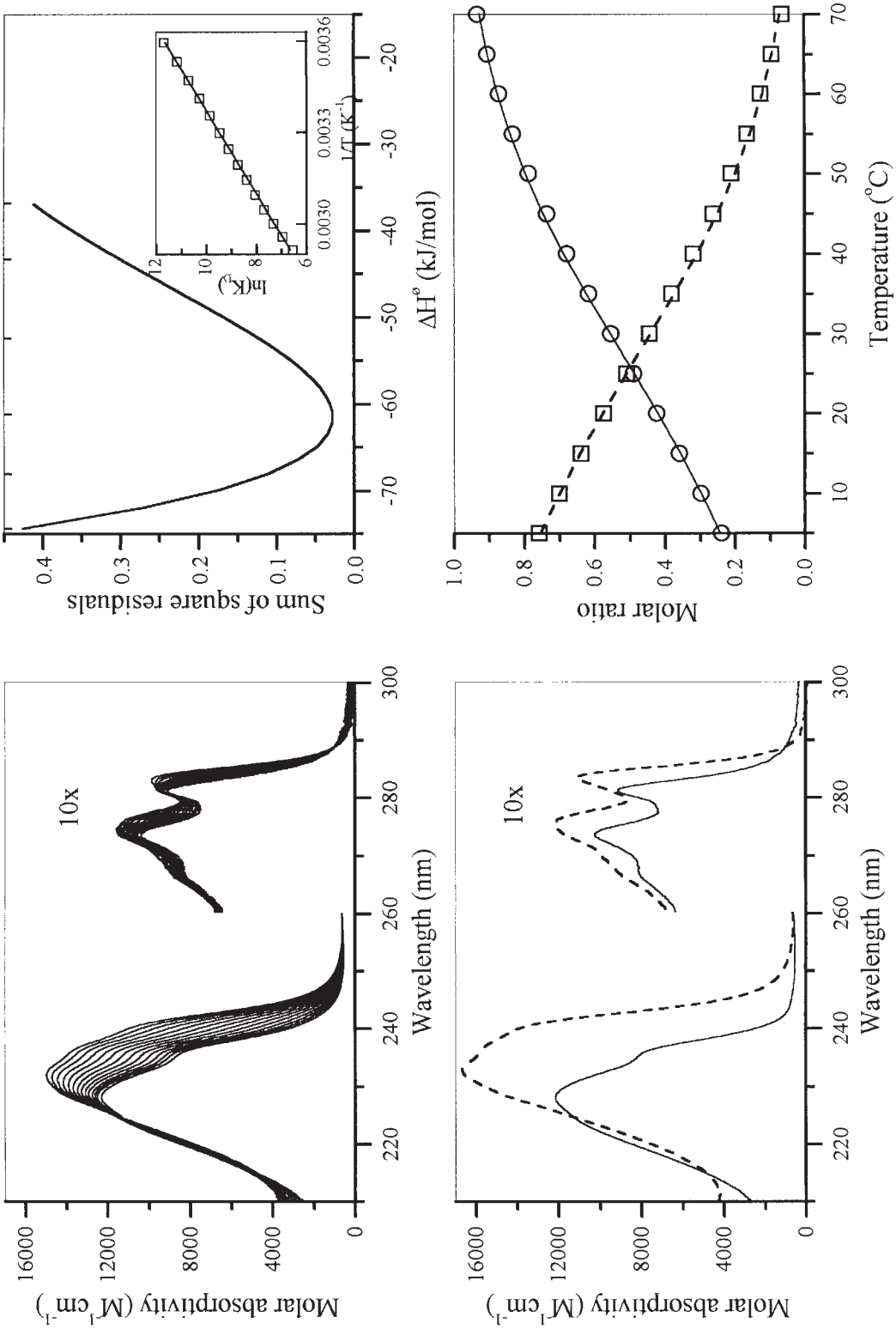

FIGURE 9. *Top left:* Absorption spectra of benzoic acid recorded at different temperatures. *Top right:* χ^2 dependence on r_{21} expressed as function of ΔH°. Inset shows the van't Hoff plot corresponding to the best fit ($\Delta H^{\circ} = -61$ kJ mol^{-1}). Calculated absorption spectra (*Bottom left*) and concentrations (*bottom right*) of the benzoic acid monomer and dimer.

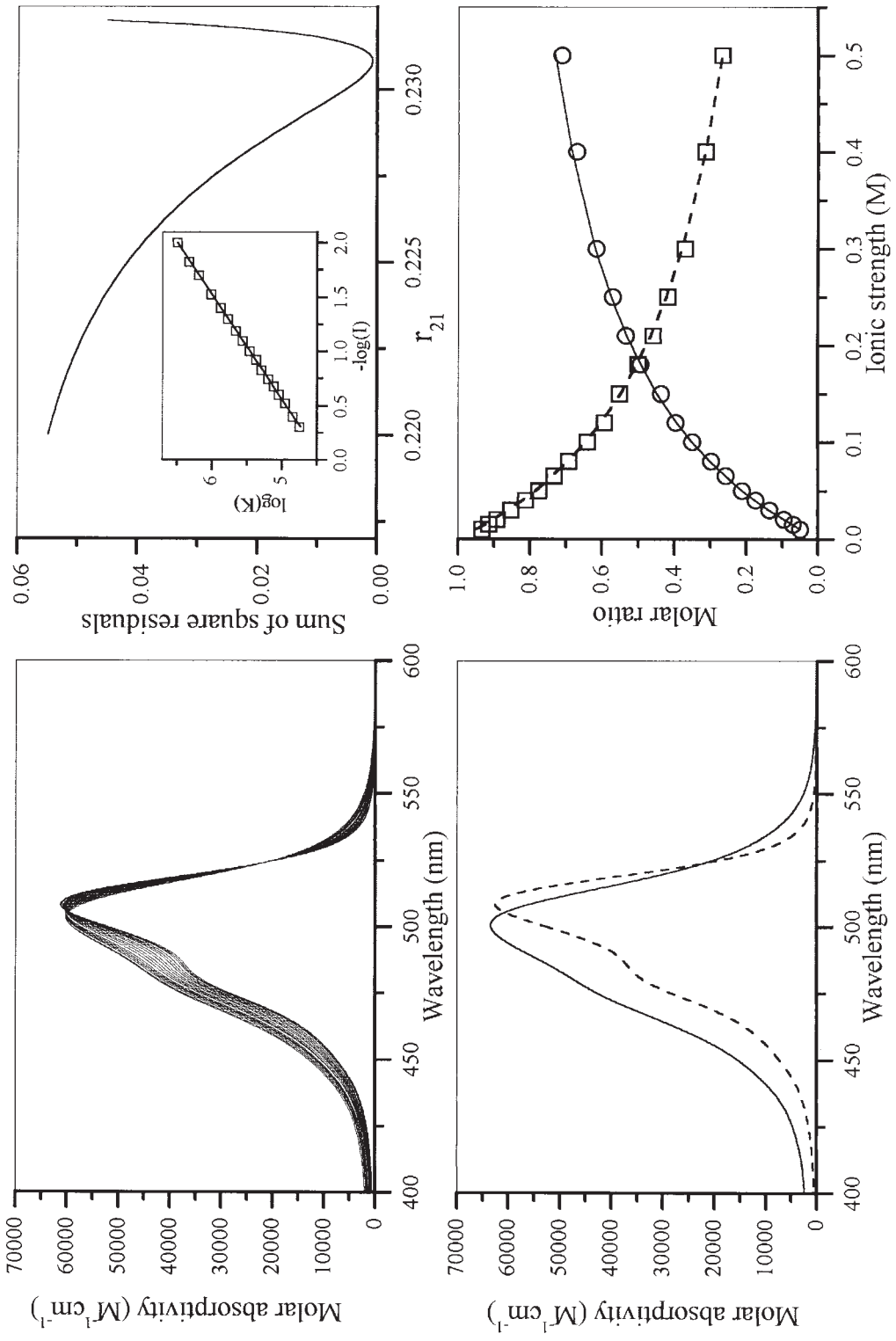

FIGURE 10. *Top left:* Absorption spectra of thiazole orange mixed with calf thymus DNA in various ionic strengths. *Top right:* χ^2 dependence on r_{21}. Inset shows a plot of log $K(I)$ vs. log I corresponding to the best fit. Calculated absorption spectra and concentrations are shown in the bottom panels.

mining the affinity of the cationic dye thiazole orange for calf thymus DNA.

E. Other Systems

Essentially, any equilibrium system that can be described in closed form can be analyzed by the physical constraint approach. Recent examples are calculation of DNA protein affinity constants by analyzing tryptophan fluorescence quenching data,[17] analyses of micellar systems,[18,19] determination of tautomeric and zwitterionic microspecies equilibrium constants,[20] and determinaton of association constants[21] and acidity constants[22] by analyzing infrared spectroscopic data.

V. PROCRUSTES ROTATION

The Procrustes rotation method does not require any *a priori* information about the sample components, and these do not have to interact. Unrelated samples with common components can be analyzed. The rotation ambiguity is here resolved by collecting correlated three-dimensional data (Figure 11). In its simplest form, one of the dimensions has only two elements. There are three principal variants that differ in the number of samples analyzed: many samples can be analyzed, each by two related 1-dimensional techniques; a pair of samples can be analyzed by an appropriate 2-dimensional technique; a single sample can be analyzed by an appropriate 3-dimensional technique.

A. Many Samples

A set of test samples with common components can be analyzed unambiguously without making assumptions about spectral shapes and other modeling by recording two spectra on each sample, such that the component contributions to the two spectra are identical in shape but of different magnitudes. Further, the response should be linear, i.e., proportional to the components' concentrations:

$$\mathbf{a}_i(\lambda) = \kappa \sum_{j=1}^{r} c_{ij}\mathbf{v}_j(\lambda) + \mathbf{e}_i^{\mathbf{a}}(\lambda) \quad (i = 1,n) \tag{50}$$

$$\mathbf{b}_i(\lambda) = \kappa \sum_{j=1}^{r} c_{ij}d_j\mathbf{v}_j(\lambda) + \mathbf{e}_i^{\mathbf{b}}(\lambda) \quad (i = 1,n) \tag{51}$$

where $\mathbf{a}_i(\lambda)$ and $\mathbf{b}_i(\lambda)$ are spectra of type A and B, respectively, recorded on sample i, c_{ij} is the concentration of component j in sample i, $\mathbf{v}_j(\lambda)$ is the spectral response of component j in measurement A, d_j is the ratio between the responses of component j in the two kind of measurements, κ is an instrument constant, and $\mathbf{e}_i^a(\lambda)$ and $\mathbf{e}_i^b(\lambda)$ contain the experimental error, which is assumed to be small. In matrix notation:

$$\mathbf{A} \approx \mathbf{CV} = \sum_{j=1}^{r} \mathbf{c}_j\mathbf{v}_j \tag{52}$$

$$\mathbf{B} \approx \mathbf{CDV} = \sum_{j=1}^{r} \mathbf{c}_j d_{jj}\mathbf{v}_j \tag{53}$$

where **A** and **B** are $(n \times m)$ matrices containing the experimental spectra as rows, **C** is an $(n \times r)$ matrix having the components concentrations as columns, **V** is an $(r \times m)$ matrix having the components spectral responses as rows and **D** is an $(r \times r)$ diagonal matrix whose elements $d_{jj} = d_j$ are the ratios between the magnitudes of the components' responses in the two measurements.

The easiest experimental design to comprehend is the combination of absorption and fluorescence measurements. In regular absorption spectroscopy, the response is given by the Beer-Lambert law, which is equivalent to Eq. 52. Rotating the detector

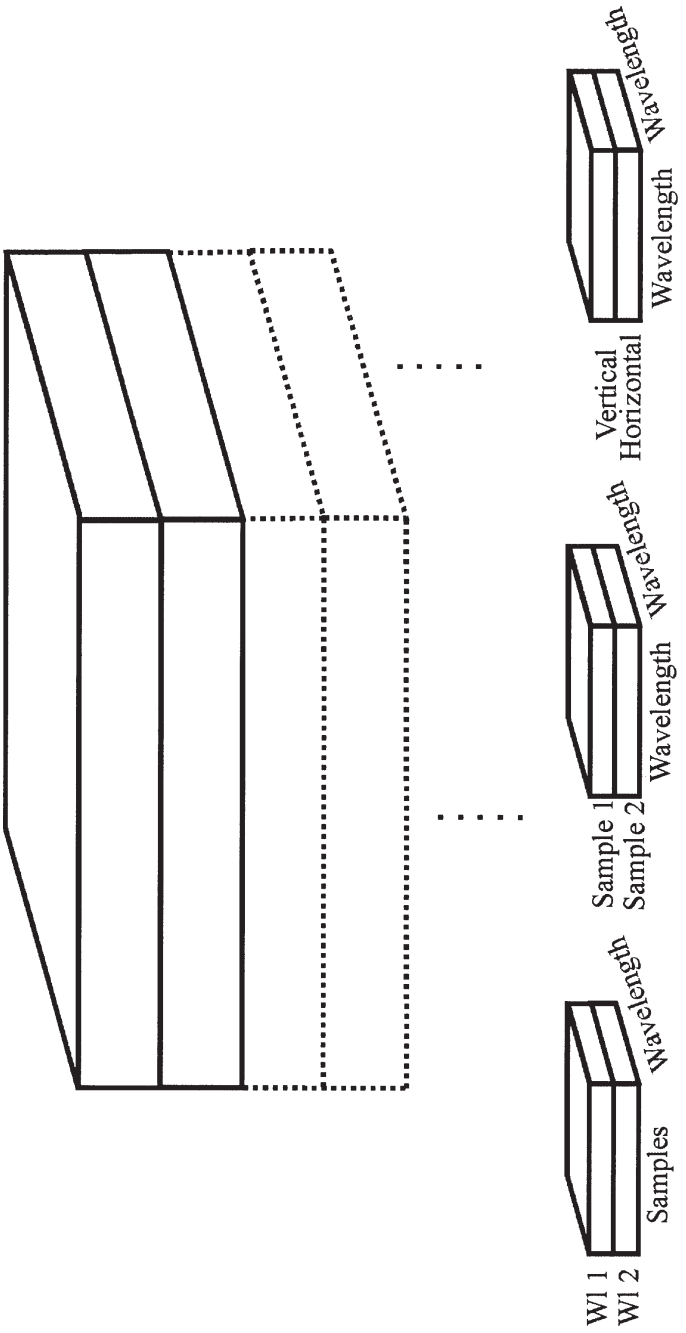

FIGURE 11. *Top:* Schematic showing the data organization required for Procrustes rotation analysis. *Bottom, left:* experimental design with many samples; *middle:* experimental design with two samples; *right:* experimental design with a single sample.

by 90° fluorescence excitation spectra are measured instead (Figure 12). Assuming that the fluorescence quantum yields are independent of excitation wavelength, the responses are given by Eq. 53, where the *d*-values are the fluorescence quantum yields of the components.

The information in the recorded spectra, contained in matrices **A** and **B**, is sufficient to determine both the spectral responses of the components (**V**), their concentrations in the samples (**C**) as well as their relative contributions to the two measurements (**D**). The data are analyzed by first laminating the matrices **A** and **B** to produce a single matrix, which is decomposed to principal components by standard procedure (Figure 13):

$$\begin{bmatrix}\mathbf{A}\\ \mathbf{B}\end{bmatrix} = \mathbf{TP}' = \begin{bmatrix}\mathbf{T}^a\\ \mathbf{T}^b\end{bmatrix}\mathbf{P}' \qquad (54)$$

The upper part of the target matrix corresponds to matrix **A** and the lower part to matrix **B**, while the projection matrix is common:

$$\mathbf{A} = \mathbf{T}^a\mathbf{P}' \qquad (55)$$

$$\mathbf{B} = \mathbf{T}^b\mathbf{P}' \qquad (56)$$

The equation system is solved by calculating the Procrustes rotation matrix, **Q**, which minimizes the difference between $\mathbf{T}^b$ and $\mathbf{T}^a$.

$$\mathbf{T}^b = \mathbf{T}^a\mathbf{Q} \qquad (57)$$

Matrix **Q** is named after the highwayman Procrustes in the Greek tale. Procrustes lived in Attica and had an iron bed that he regarded as the standard length because it just fit him. He provided travelers with lodging and during night tied them to the bed. If the person happened to be too short, Procrustes stretched him until he attained the correct length, and if he happened to be too long his legs were cut. Thus, everyone was made identical in size.

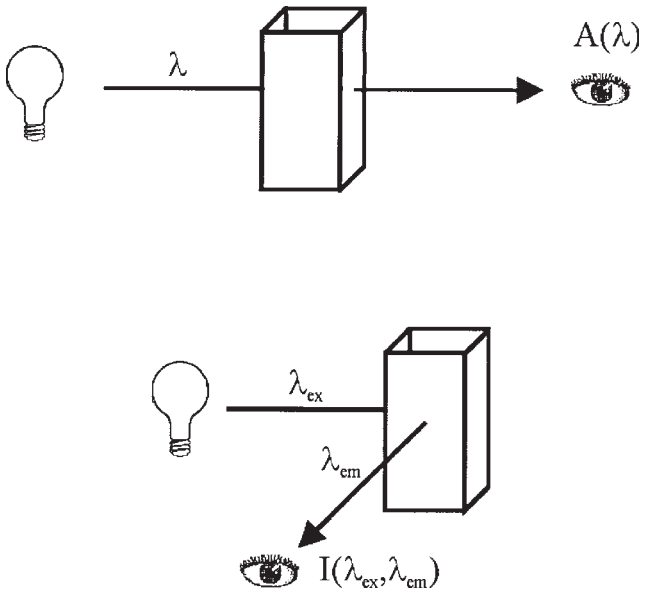

FIGURE 12. Set up for absorption (*top*) and fluorescence excitation (*bottom*) measurement.

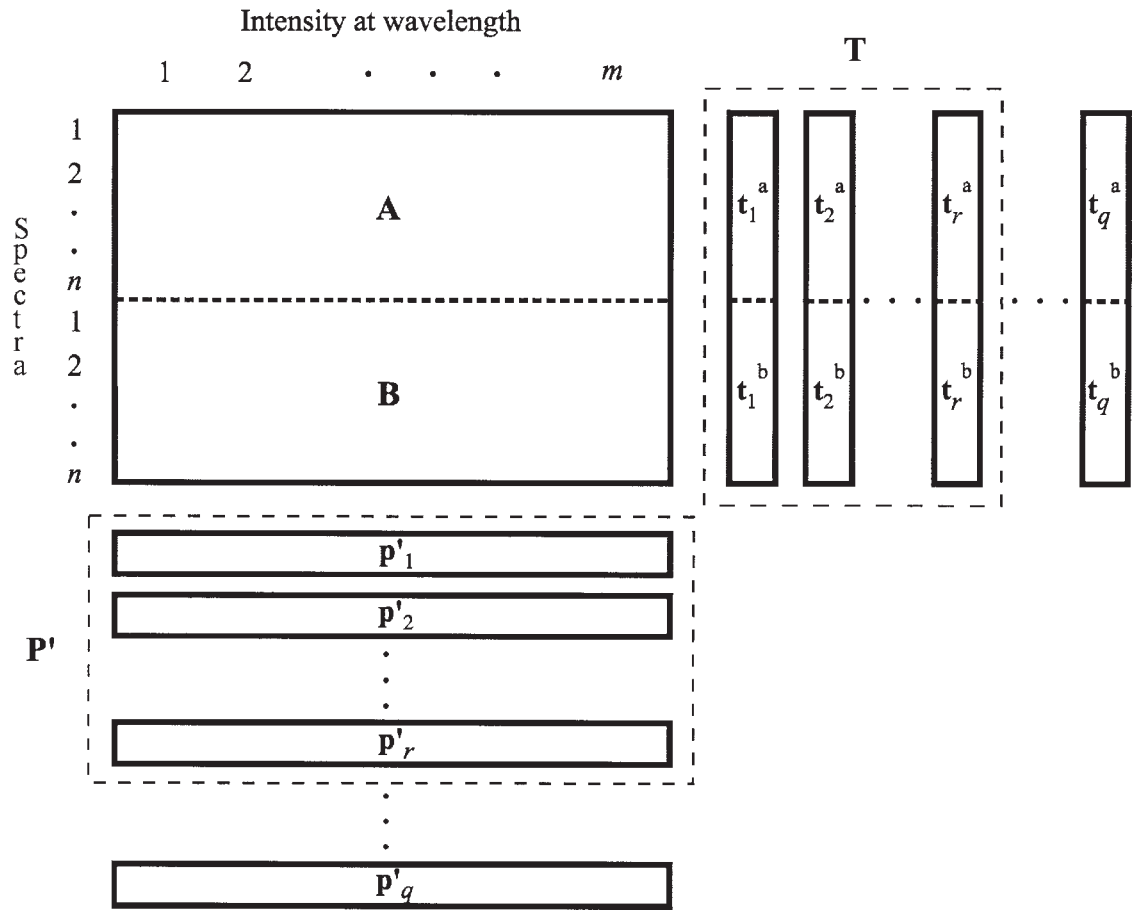

FIGURE 13. Schematic representation of the principal component decomposition of the laminated data matrix $\begin{bmatrix}\mathbf{A}\\ \mathbf{B}\end{bmatrix}$ into a product of a target (**T**) and a projection (**P′**) matrix.

The Procrustes rotation matrix is calculated by the least square method.

$$\mathbf{Q} = \left(\left(\mathbf{T}^{a}\right)'\mathbf{T}^{a}\right)^{-1}\left(\mathbf{T}^{a}\right)'\mathbf{T}^{b} \qquad (58)$$

Because the projection vectors are orthonormal

$$\mathbf{P}'\mathbf{P} = \mathbf{I} \qquad (59)$$

where **I** is the $(r \times r)$ identity matrix. Equations 52, 53, 55, and 56 give

$$\mathbf{T}^{a} = \mathbf{AP} = \mathbf{CVP} \qquad (60)$$

$$\mathbf{T}^{b} = \mathbf{BP} = \mathbf{CDVP} \qquad (61)$$

Introducing the rotation matrix **R**,

$$\mathbf{C} = \mathbf{T}^{a}\mathbf{R}^{-1} \qquad (62)$$

$$\mathbf{V} = \mathbf{RP}' \tag{63}$$

gives

$$\mathbf{DR} = \mathbf{DVP} = (\mathbf{C}'\mathbf{C})^{-1}\mathbf{CT}^{b} = (\mathbf{C}'\mathbf{C})^{-1}\mathbf{CT}^{a}\mathbf{Q} = \mathbf{VPQ} = \mathbf{RQ} \tag{64}$$

Transposing both sides

$$\mathbf{R}'\mathbf{D} = \mathbf{Q}'\mathbf{R}' \tag{65}$$

where $\mathbf{D}' = \mathbf{D}$. Because **D** is diagonal this is a nonsymmetrical eigenvalue equation that is solved by diagonalizing $\mathbf{Q}'$. This determines matrix **D** as well as matrix **R**, from which matrices **C** and **V** are calculated. Matrix **D** is determined absolutely, while matrices **C** and **V** must be normalized.[4]

The combination of absorption and fluorescence excitation spectra has the technical disadvantage that different instruments are used for the two measurements, which leads to errors owing to inaccurate wavelength calibrations and instrument non-linearity. It is preferable to analyze pairs of excitation spectra, i.e., two excitation spectra recorded at different emission wavelengths on each sample, or pairs of emission spectra recorded at different excitation wavelengths. In Figure 14, emission spectra of fluorescein recorded at two different excitation wavelengths at various pH in the range 5.4 to 7.9 are shown. The spectra are described by:

$$\mathbf{I}(\lambda_{em})_{pH}^{ex1} = \kappa \sum_{j=1}^{r} c_j^{pH} I_j(\lambda_{ex1}) \mathbf{I}_j(\lambda_{em}) \tag{66}$$

$$\mathbf{I}(\lambda_{em})_{pH}^{ex2} = \kappa \sum_{j=1}^{r} c_j^{pH} I_j(\lambda_{ex2}) \mathbf{I}_j(\lambda_{em}) \tag{67}$$

In matrix notation

$$\mathbf{M}_{ex1} = \kappa \mathbf{C}\mathbf{X}_{ex1}\mathbf{M} \tag{68}$$

$$\mathbf{M}_{ex2} = \kappa \mathbf{C}\mathbf{X}_{ex2}\mathbf{M} \tag{69}$$

where $\mathbf{M}_{ex1}$ and $\mathbf{M}_{ex2}$ contain the recorded emission spectra, **C** contains the concentrations of the components, $\mathbf{X}_{ex1}$ and $\mathbf{X}_{ex2}$ contain the normalized excitation intensities and **M** contains their normalized emission spectra. κ is an instrument constant. Renormalizing

$$\mathbf{M}_{ex1} = \mathbf{CM} \tag{70}$$

$$\mathbf{M}_{ex2} = \mathbf{CXM} \tag{71}$$

C now contains the components' emission spectra scaled by their excitation intensities in the first measurement and **X** is a diagonal matrix containing the ratios between the components' excitation intensities at the two excitation wavelengths used:

$$x_{jj} = \frac{I_j(\lambda_{ex2})}{I_j(\lambda_{ex1})} \tag{72}$$

PCA revealed that two components contribute to the spectra, which are the mono and dianion, and by Procrustes rotation their emission profiles and concentrations were calculated (Figure 14), as well as the ratios between their excitation intensities

$$\left(I_{Fl^{2-}}(\lambda_{ex2}) \big/ I_{fl^{2-}}(\lambda_{ex1}) = 3.0 \text{ and } I_{HFl^{-}}(\lambda_{ex2}) \big/ I_{HFl^{-}}(\lambda_{ex1}) = 1.5\right)$$

B. Pairs of Samples

Procrustes rotation can also be used to analyze a pair of samples, for example, by recording emission spectra at a large number of excitation wavelengths, or by recording excitation spectra at a number of emission wavelengths. Figure 15 shows emission spectra recorded at many excitation wavelengths of fluorescein samples at pH 5.56 and 6.53. The spectra are described by:

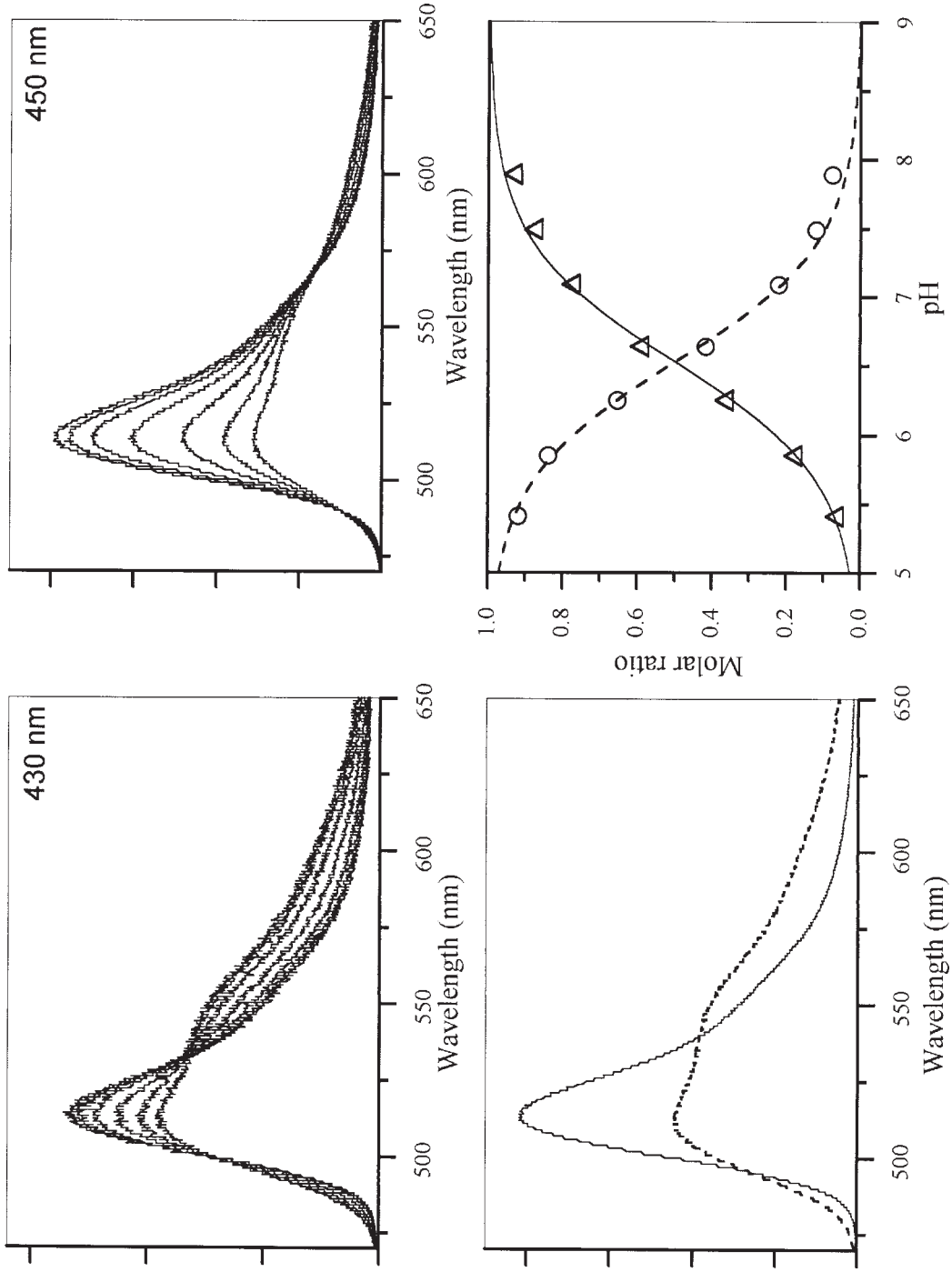

FIGURE 14. *Top:* Emission spectra of fluorescein recorded on samples with different pH using 430 nm (*left*) and 450 nm (*right*) excitation. *Bottom:* Calculated emission spectra (*left*) and molar ratios (*right*) of the fluorescein monoanion and dianion.

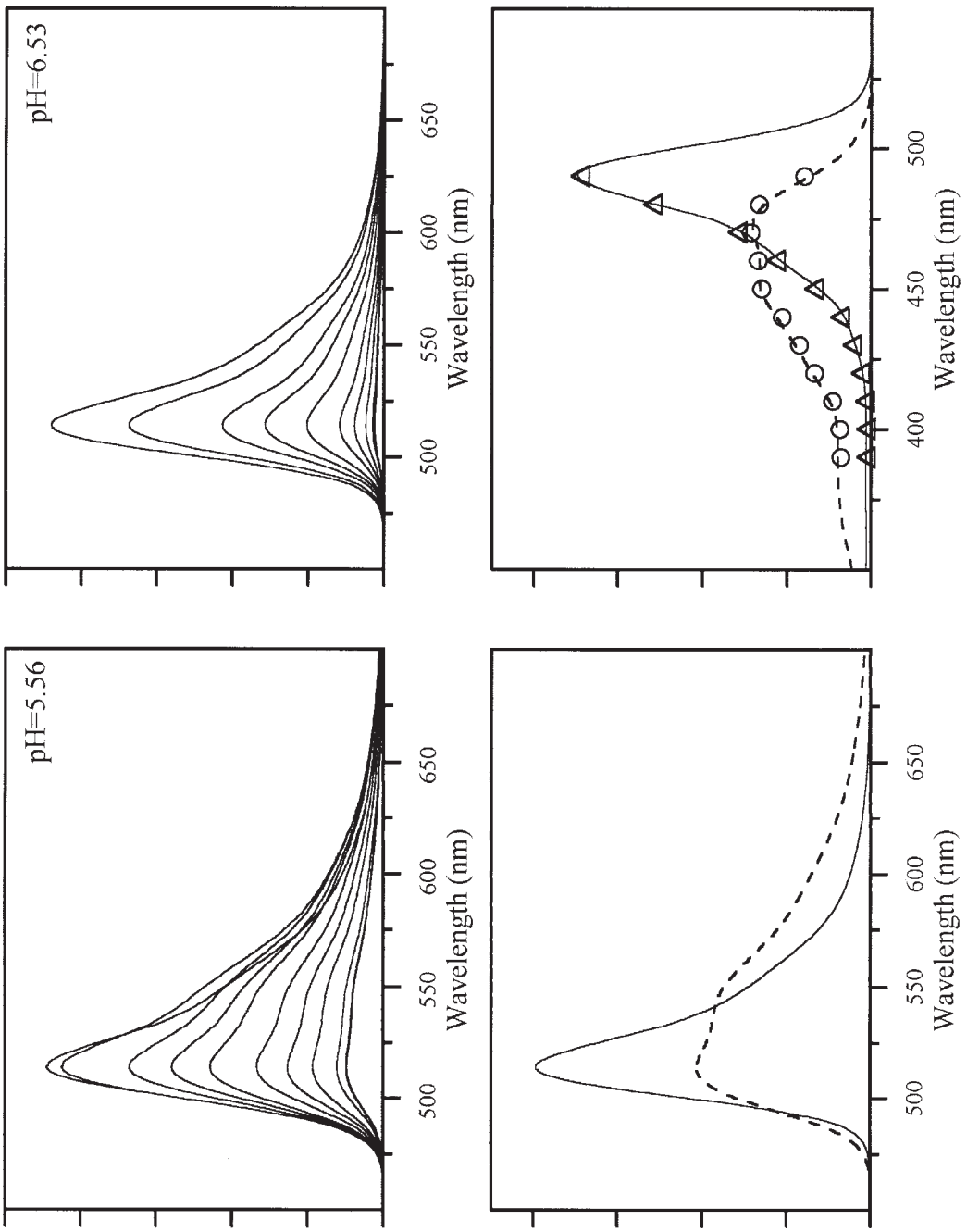

FIGURE 15. *Top:* Emission spectra of fluorescein recorded at different excitation wavelengths on two samples having the pH 5.56 (*left*) and 6.53 (*right*). *Bottom:* Calculated emission spectra of the fluorescein monoanion and dianion (*left*) and their calculated excitation intensities (*right*). For comparison, separately determined excitation spectra are shown.

$$\mathbf{I}(\lambda_{em})_{ex}^{pH1} = \kappa \sum_{j=1}^{r} I_j(\lambda_{ex}) c_j^{pH1} \mathbf{I}_j(\lambda_{em}) \quad (73)$$

$$\mathbf{I}(\lambda_{em})_{ex}^{pH2} = \kappa \sum_{j=1}^{r} I_j(\lambda_{ex}) c_j^{pH2} \mathbf{I}_j(\lambda_{em}) \quad (74)$$

In matrix notation

$$\mathbf{M}_{pH_1} = \kappa \mathbf{X} \mathbf{C}_{pH_1} \mathbf{M} \quad (75)$$

$$\mathbf{M}_{pH_2} = \kappa \mathbf{X} \mathbf{C}_{pH_2} \mathbf{M} \quad (76)$$

where matrices **X** and **M** contain the normalized excitation and emission spectra of the components, and the diagonal **C** matrices contain the components' concentrations in the two samples. Renormalizing

$$\mathbf{M}_{pH_1} = \mathbf{X}\mathbf{M} \quad (77)$$

$$\mathbf{M}_{pH_2} = \mathbf{X}\mathbf{C}\mathbf{M} \quad (78)$$

C now contains the ratios between the components' concentrations in the samples

$$c_{jj} = \frac{c_j^{pH_2}}{c_j^{pH_1}} \quad (79)$$

PCA revealed the presence of two components, and by Procrustes rotation their excitation and emission spectra were calculated (Figure 15), as well as their concentration ratios

$$\left(c_{Fl^{2-}}^{pH_2} / c_{Fl^{2-}}^{pH_1} = 4.5 \text{ and } c_{HFl^{-}}^{pH_2} / c_{HFl^{-}}^{pH_1} = 0.48 \right)$$

Successful Procrustes rotation analysis requires that all the elements in the diagonal matrix are different, so additional samples cannot be generated by dilution. However, a single sample can be split into aliquots with unequal relative components' concentrations by, for example, solvent extraction. Hence, one can start with a single test sample, split it into two aliquots and determine the spectra of its components from which they can be identified.[7]

C. A Single Sample

It is also possible to identify the components directly in a single test sample by an appropriate 3-dimensional measurement. This is illustrated in Figure 16, where fluorescence excitation/emission scans were recorded on a single sample using vertically and horizontally polarized light. Two components were found by PCA, and their spectra were calculated by Procrustes rotation.

A single sample can also be analyzed by NMR measurements, as shown by Schulze and Stilbst.[23] They analyzed a sample in NMR self-diffusion measurements by varying the amplitude of the gradient pulses and the magnetic field. By also using different gradient pulses, two data sets were generated and Procrustes analysis could be performed. By utilizing that the signal response is exponential, Antalek and Windig[25] showed that the two required data sets for Procrustes rotation analysis could be generated from a single experimental set by shifting the intensities along the measurement dimension:

$$\mathbf{a}_i(x) = \sum_{j=1}^{r} c_{ij} \mathbf{e}^{-k_j x} \quad (80)$$

$$\mathbf{b}_i(x) = \mathbf{a}_i(x+\Delta) = \sum_{j=1}^{r} c_{ij} \mathbf{e}^{-k_j (x+\Delta)} = \sum_{j=1}^{r} c_{ij} \mathbf{e}^{-k_j x} \mathbf{e}^{-k_j \Delta} \quad (81)$$

From the experimental data, $\mathbf{a}_i(x)$, both the components concentrations, c_{ij}, and decay constants, k_j, are determined. The approach was recently applied in the analysis of magnetic resonance 2D images.[25]

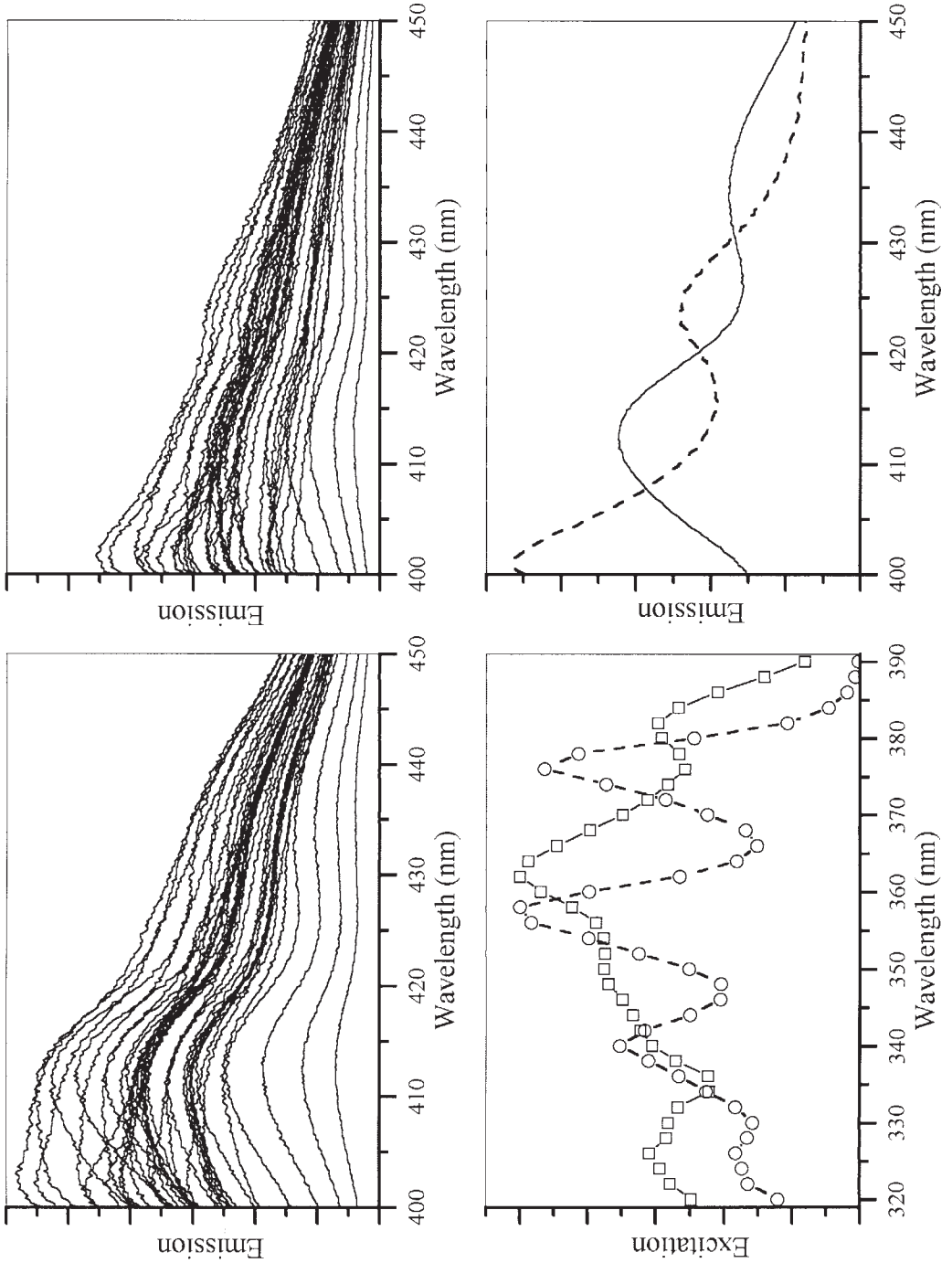

FIGURE 16. *Top:* Emission spectra, of a single sample containing anthracene and POPOP in mineral oil, collected at different excitation wavelengths using parallel (*left*) and perpendicular (*right*) polarized light. *Bottom:* Calculated excitation intensities (*left*) and calculated emission spectra (*right*).

D. Generalized Procrustes Rotation

So far, we have only discussed cases where one of the three dimensions in Procrustes rotation analysis has exactly two elements, which is sufficient to obtain a unique solution. However, one can readily collect data with many elements in each dimension. For example, by recording excitation/emission scans of samples at many different pH. The analysis of such large data sets is, however, nontrivial, because the regular Procrustes rotation approach cannot be used. Liwo´s group recently developed a procedure based on finding initial conditions for a general global minimization using the Procrustes approach.[26] They tested the analysis on fluorescence spectra collected from several samples and indeed found that highly accurate solutions were obtained. Although the approach is stable, finding the global minimum took several hours on a standard personal computer for a typical data set. A new mathematical algorithm to solve this problem was recently developed by Ibraghimov.[27,28] The number of arithmetic operations is proportional to the number of independent chemical species present, instead of being proportional to the number of samples as in Liwos algorithm, resulting in reasonable execution times with most data sets.

E. Reaction Kinetics, Decay Kinetics, and Chromatography Data

Procrustes rotation can also be applied to kinetic data. For example, monitoring stopflow kinetics by diode-array fluorescence detection, using (at least) two excitation wavelengths, components' spectral responses, and their kinetic profiles, including those of intermediate species, can be determined without making model assumptions. Similar approaches can be used to analyze chromatographic data. Recording fluorescence spectra at two excitation wavelengths at each time point, the contribution from the components can be separated without making assumptions about spectral responses or shapes of elution profiles. Procrustes rotation is also expected to be valuable for analysis of decay kinetics, such as fluorescence decays. Recording time-resolved fluorescence emission spectra at two excitation wavelengths, it is possible to determine both the emission spectra and intensity decays of all components including intermediate species, without making model assumptions. No such applications have yet been described though, but we expect them to become important in the future.

SUMMARY

Chemometric methods that compare measured spectra with those of standards are today commonly used to solve problems in research and in industry. Here we show that even when the spectra of the components are not known, successful analysis is possible. Depending on the dimensionality of the experimental data, the physical constraint approach or Procrustes rotation can be used to calculate the spectra and the relative concentrations of the components.

REFERENCES

1. Lawton, W.; Sylvestre, E. *Technometrics* **1971**, 13, 617–633.
2. Ohta, N. *Anal. Chem.* **1973**, 45, 553–557.
3. Kubista, M. *Chemom. Intell. Lab. Syst.* **1990**, 7, 273–279.
4. Scarminio, I.; Kubista, M. *Anal. Chem.* **1993**, 65, 409–416.
5. Sanches, E.; Kowalski, B. R. *Anal. Chem.* **1986**, 58, 496–499.
6. Sjöback, R.; Nygren, J.; Kubista, M. *Spectro. Acta Part A* **1995**, 51, L7-L21.

7. Nygren, J.; Abdalla, E.; Kubista, M. *Anal. Chem.* **1998**, 70, 4841–4846.
8. Kubista, M.; Sjöback, R.; Albinsson, B. *Anal. Chem.* **1993**, 65, 994–998.
9. Kubista, M.; Sjöback, R.; Nygren, J. *Anal. Chim. Acta.* **1995**, 302, 121–125.
10. Nygren, J.; Andrade, J.; Kubista, M. *Anal. Chem.* **1996**, 68, 1706–1710.
11. Wold, S. *Chemom. Intell. Lab. Syst.* **1987**, 2, 37–52.
12. Elbergali, A.; Nygren, J.; Kubista, M. *Anal. Chim. Acta* **1999**, 379, 143–158.
13. Wold, H.; Lyttkens, E. *Bulletin of the International Statistical Institute Proceedings* **1969**, 37, 1.
14. Eriksson, E.; Kim, S. K.; Kubista, M.; Nordén, B. *Biochemistry* **1993**, 32, 2987–2998.
15. Record, M. T.; Lohman, T. M.; De Haseth, P. *J. Mol. Biol.* **1976**, 107, 145–158.
16. Nygren, J.; Svanvik, N.; Kubista, M. *Biopolymers* **1998**, 46, 39–51.
17. Sjöback, R.; Gustafsson, C. M.; Kubista, M. *J. Luminescence.* **1997**, 72, 610–611.
18. Vitha, M. F.; Weckwerth, J. D.; Odland, K.; Dema, V.; Carr, P. W. *Anal. Chem.* **1997**, 69, 2268–2274.
19. Vitha, M. F.; Carr, P. W. *J. Phys. Chem. B* **1998**, 102, 1888–1895.
20. D'Angelo, J. C.; Collette, T. W. *Anal. Chem.* **1997**, 69, 1642–1650.
21. Nissink, W. J. M.; Boerrigter, H.; Verboom, W.; Reinhoudt, D. N.; van der Maas, J. H. *J. Chem. Soc.-Perk. Trans. 2* **1998**, 7, 1671–1675.
22. Barja, B. C.; Afonso, M. D. *Envir. Sci. Tech.* **1998**, 32, 3331–3335
23. Schulze, D.; Stilbs, P. *J. Magn. Res. Ser. A* **1993**, 105, 54–58.
24. Antalek, B.; Windig, W. *J. Am. Chem. Soc.* **1996**, 118, 10331–10332.
25. Windig, W.; Hornak, J. P.; Antalek, B. *J. Magn. Res.* **1998**, 132, 298–306.
26. Liwo, A.; Skurski, P.; Oldziej, S.; Lankiewicz, L.; Malicka, J.; Wiczk, W. *Computers Chem.* **1997**, 2, 89–96.
27. Ibraghimov, I. V. in *Matrix Methods and Algorithms*; INM RAS: Moscow, 1998.
28. Ibraghimov, I. V.; Elbergali, A.; Nygren, J.; Kubista, M. submitted **1999**.